Materials Horizons

Performance-oriented multistage design for multi-principal element alloys with low cost yet high efficiency

Journal:	*Materials Horizons*
Manuscript ID	MH-COM-11-2021-001912.R2
Article Type:	Communication
Date Submitted by the Author:	09-Mar-2022

Complete List of Authors:	Li, Jia; Hunan University, State Key Laboratory of Advanced Design and Manufacturing for Vehicle Body Xie, Baobin; Hunan University, Li, Li; Hunan University Liu, Bin; Central South University, Liu, Yong; Central South University, Sate Key Laboratory of Powder Metallurgy Shaysultanov, Dmitry; National Research University Belgorod State University Fang, Qihong; Hunan University Stepanov, Nikita; National Research University Belgorod State University Liaw, Peter K.; University of Tennessee Knoxville,

Energy shortage and environmental pollution have been great challenges so far for human beings. Here, we report a highly effective, precise, and environmentally friendly material design strategy through a novel machine learning approach integrating the physical laws and mathematical model, which is successfully applied to the development of complex multi-phase multi-principal element alloys (MPEAs), contributing to the world's carbon neutrality process. Here, a feasible material design avenue is proposed by integrating the machine learning, physical law, and mathematical model. A new developed MPEA with a good combination of strength and plasticity exceeding that of its system and subsystems reported so far is then screened and prepared within only two days. It has been demonstrated that the efficiency and economy of the present work are several hundred times higher than those of the existing approach. Most importantly, the present work provides a universal framework for the precise and rapid tailor of the property-guided composition and microstructure, which further broadens the applicable scope of advanced MPEAs.

Performance-oriented multistage design for multi-principal element alloys with low cost yet high efficiency

Jia Li[a1], Baobin Xie[a1], Li Li[a1], Bin Liu[b], Yong Liu[b], Dmitry Shaysultanov[c], Qihong Fang[a*], Nikita Stepanov[c*], and Peter K. Liaw[d]

[a] *State Key Laboratory of Advanced Design and Manufacturing for Vehicle Body, College of Mechanical and Vehicle Engineering, Hunan University; Changsha, 410082, PR China*

[b] *State Key Laboratory of Powder Metallurgy, Central South University; Changsha, 410083, PR China*

[c] *Laboratory of Bulk Nanostructured Materials, Belgorod State University; Belgorod, 308015, Russia*

[d] *Department of Materials Science and Engineering, The University of Tennessee; Knoxville, TN 37996, USA*

[1] *These authors contributed equally to this work.*

* *Corresponding author. E-mail address:* fangqh1327@hnu.edu.cn (Q.H. Fang), and stepanov@bsu.edu.ru (N. Stepanov).

Abstract

Multi-principal element alloys (MPEAs) with remarkable performances possess a great potential as structural, functional, and smart materials. However, their efficient performance-orientated design in a wide range of compositions and types is an extremely-challenging issue, because of properties strongly dependent upon the composition and composition-dominated microstructure. Here, we propose a multistage-design approach integrating machine learning, physical law and mathematical model for developing the desired-property MPEAs in a very time-efficient way. Compared to existing physical model- or machine-learning-assisted material development, the forward-and-inverse problems, including identifying the target property and unearthing the optimal composition, can be tackled with better efficiency and higher accuracy using our proposed avenue, which defeats one-step component-performance design strategy by multistage-design coupling constraints. Furthermore, we developed a new multi-phase MPEA at the minimal time and cost, whose high strength-ductility synergy exceeding those of its system and subsystem reported so far by searching for the optimal combination of phase fraction and composition. The present work suggests the property-guided composition and microstructure are precisely tailored through the newly-built approach with significant reductions of the development period and cost, which is readily extendable to other multi-principal element materials.

Introduction

Obtaining multi-principal element alloys (MPEAs) with excellent mechanical properties through traditional trial-and-error methods is an extremely time- and cost-consuming task, owing to the near-infinite compositional space and its impact on phase structures.[1-9] Despite the involvement of multi-scale simulation tools and high-throughput technologies,[10-12] the precise design of MPEAs with desired properties is still a challenge due to the complicated process producing the complex and uncertain microstructures. Naturally, it is crucial to search for an effective and accurate strategy/approach to predict the structures/properties and design the desired-performance MPEA system. Recently, machine learning has been actively promoted for the development of phase selection, performance prediction, and component screening in MPEAs.[13-15] Nevertheless, the conventional data-driven machine learning models have so far neglected the physical essence of the problems and caused less explainable and poor generalization. Indeed, the existing machine learning models,[16, 17] which are still in their infancy for the computer-aided material design, have been limited to numerically establishing the connection between input/output features. The deep integration of the physical cognition and machine learning has not yet been enforced to the development of MPEAs. Here, we provide a universal multistage design framework, by which we successfully design a new multi-phase MPEA. Comparing the tensile properties of this MPEA with its system and subsystems proposed in the literature, it is demonstrated that the present MPEA possesses superior combinations of yield strength and elongation.

To develop the multi-phase MPEAs with the excellent properties fastly and accurately, a multistage design method integrating the physical law, mathematical model, and machine

learning is presented in Fig. 1A. Hence, two core problems should be solved, namely both the forward problem (FP) avenue (from the composition to desired performance) and the inverse problem (IP) avenue (from the target performance to optimal composition), as shown in Fig. 1B. Here, the multistage strategy has been embedded in the FP and IP avenues, which is composed of two parts, introducing a composition dependent physics feature space to predict phase formation, and a phase dependent mathematical model to calculate yield strength. In order to obtain the target performance, we can screen out the initial composition space, and then determine the optimal composition (Fig. 1B). Compared to the results of the one-step strategy, this work can rapidly converge in the desired region, resulting in the reduction of the experimental trial and error, no matter in the FP avenue or the IP avenue. Thus, the current novel approach can effectively reduce development cycle and resource consumption in complicated materials.

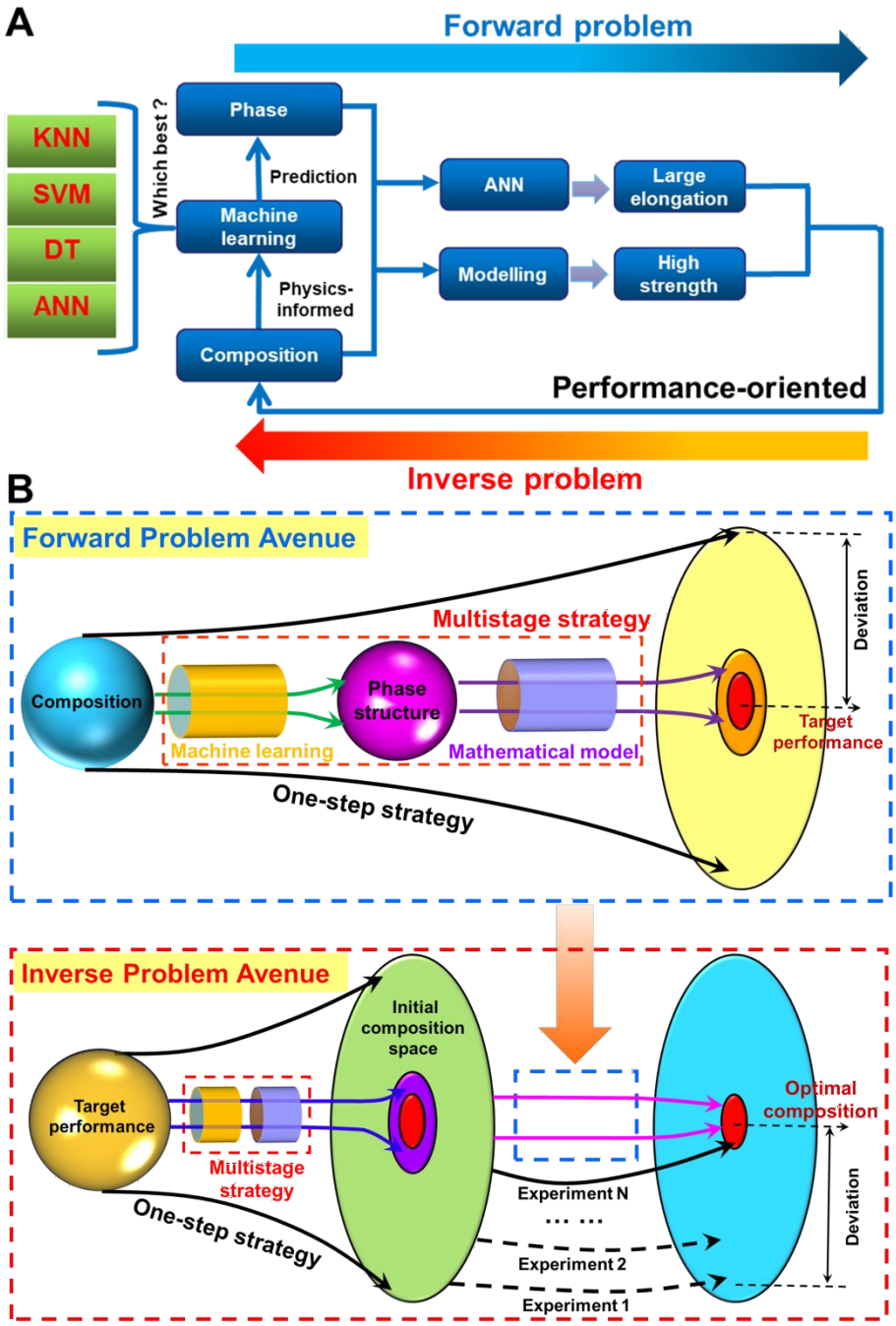

Figure 1. Strategy of the multistage design for the performance-oriented precision design. (A) Flowchart of optimization design in multi-phase MPEAs with high strength and large elongation. Several common machine learning algorithms, including K-nearest neighbors (KNN), decision tree (DT), support vector machine (SVM), and artificial neural network (ANN) are used to predict the phase selection of MPEAs. Here, the widely-studied physics-based features for the phase formation of MPEA are calculated as the initial input features (a detailed description in Table S1). (B) The comparisons of the one-step and multistage strategies in FP and IP avenues. The black arrows represent the process of one-step

strategy. The colored arrows denote the process of multistage strategy.

Experimental section

Sample preparation

Two alloys with a nominal composition of $Al_{0.63}Co_{0.95}Cr_{0.95}FeMn_{0.74}Ni$ and $Al_{0.55}Co_{0.9}CrFe_{0.95}Mn_{0.8}Ni_{0.8}$ (mole fraction) were produced by vacuum arc melting. High-purity (at least 99.5 weight percent, wt.%) powders of the constitutive elements were used as starting materials. The produced ingots had dimensions of ~ 10 × 14 × 50 mm^3. The ingots were remelted 5 times to ensure the chemical homogeneity. The SEM-EDS analysis showed that the actual chemical composition of the alloy closely corresponded to the nominal one.

Microstructural characterization

The microstructure and phase composition of the alloys in the as-cast condition were studied, using X-ray diffraction (XRD), scanning electron microscopy (SEM), and transmission electron microscopy (TEM) techniques. The XRD analysis was performed, using a RIGAKU diffractometer and Cu Kα radiation. Samples for the SEM observations were prepared by careful mechanical polishing. The SEM investigations were performed employing a FEI Quanta 300 3D and a FEI Nova NanoSEM microscope equipped with a back-scattered electron (BSE), an energy-dispersive X-ray spectrometry (EDS), and an electron backscattered diffraction (EBSD) detectors. The EBSD phase maps were produced, utilizing a TSL OIM software. Samples for TEM analysis were prepared by the conventional twin-jet electro-polishing of mechanically pre-thinned to 100 μm foils, in a mixture of 95% C2H5OH and 5% HClO4 at the 27 V potential. The TEM investigations were performed,

employing a JEOL JEM-2100 microscope equipped with an EDS detector at an accelerating voltage of 200 kV.

Mechanical testing

Tensile mechanical tests were performed, utilizing an Instron 5882 machine. Dog-bone specimens with gauge dimensions of 1.5 × 3 × 5 mm^3 for testing were cut, using an electric discharge machine. Prior to testing, the specimens were carefully mechanically polished. Tensile testing to fracture was carried out at an initial strain rate of 10^{-3} s^{-1}. Elongation to fracture was determined by a VIC-3D system. 3 tests were performed to ensure the consistency of the results.

Mathematical modeling

The mathematical modeling is a very important bridge to relate fundamental material properties to macroscopic material behavior. Here, the fundamental properties (such as composition and elastic moduli) are connected to specific mechanisms of deformation (such as dislocation slip and phase structure), which then collectively determine the macroscopic properties (such as strength and strain hardening). In MPEAs, the yield strengths can be composed of the grain-boundary strengthening and lattice-friction stress. The grain-boundary strengthening in MPEAs is supposed to be similar to that in traditional alloys.[18] However, the lattice-friction stress in MPEAs is significantly different from that in traditional alloys, owing to their intrinsic multi-principal characteristics. Here, we utilize the lattice-distortion-introduced stress originating from the atomic difference between various multi-principal elements in MPEAs to replace the sum of the solid-solution strengthening and lattice-friction stress in traditional alloys, owing to the fact that there is no definite distinction

between the solute and solution in MPEAs. It is noted that the present model contains no fitting parameters. The computed inputs are the compositions and phase structures of the MPEAs, where the former is the inherent feature of materials, and the latter can be obtained by the machine learning approach. The detailed calculation description of yield strength is provided in Supplementary Text 1 "Yield strength of MPEAs". Here, the proposed mathematical model can directly calculate the yield strength of single phase MPEAs. For the dual-phase MPEAs, their yield strength is predicted through the mixing theory, which needs the phase volume fraction calculated based on the constructed "composition-FCC/BCC volume fraction" model by machine learning (Supplementary Text 2).

Data collection

The initial "composition-phase structure" data set is built by collecting the available experimental results in the previous literature (a detailed alloy composition and the corresponding source in Data S1), including 325 entries with some common MPEA systems, like Al-Fe-Co-Cr-Ni-Mn, Co-Cr-Fe-Ni, and Mo-Nb-Ta-V-Zr. Furthermore, considering that process parameters have significant influence on the microstructure and properties, the MPEAs collected in the initial data set were all prepared by arc melting to prevent measurement differences. The data set includes three MPEAs phase structures (BCC, BCC+FCC, and FCC). In view of few HCP MPEAs so far, the HCP MPEAs are excluded for avoiding unbalanced data distribution. In addition, to ensure the reliability of the data set and improve the accuracy and efficiency of machine learning model, data cleaning is a critical step before using machine learning algorithms. The basic guideline is that each MPEA composition corresponds to a unique phase and each item appears only once. Besides, all of

the entries with the same composition yet the different phase structures induced by the variation of process parameters need to be excluded because the accuracy of these data can not be figured out. Meanwhile, some obviously outlier entries are removed by observing the distribution of input features (detailed description about input features in Data analysis). After data cleaning, the final data set for phase prediction is composed of 266 entries with 103 BCC, 61 FCC and 102 BCC + FCC phases (Data S2).

Machine learning algorithm

The performance of the four machine learning algorithms, including KNN algorithm, DT algorithm, SVM algorithm, and ANN algorithm, are evaluated in the current work. In order to protect against the over-fitting issue when using machine learning algorithms, five-folds cross-validation method is used for KNN, DT, and SVM algorithms while an early-stopping strategy is adopted for the ANN algorithm. The descriptions of these machine learning algorithms, five-folds cross-validation method and early-stopping strategy are elaborated in Supplementary Text 1 “Machine learning algorithm”.

Results and discussion

Data analysis

Before the implementation of the machine learning algorithms, it is critical to determine the appropriate descriptors as the input features. Apparently, it is unreasonable to use the elements and corresponding composition fraction as descriptors because of the unpredictable dimensional disaster and excessive computation. Luckily, Hume-Rothery rules[19] denote that some physical features, such as the valence electron concentration (VEC), mixing entropy (ΔS_{mix}), mixing enthalpy (ΔH_{mix}), atomic-size difference (δ) and electronegativity difference

($\Delta\chi$), are closely related to the phase formation of MPEAs. Based on the previous work, some other important physics features, such as thermodynamics features[20] (average melting temperature T_m, and thermal stability parameters Ω), atomic features[21] (γ), physical properties (elastic modulus *E*, bulk modulus *B*, and alloy density ρ) as well as hybrid feature[22] (λ), are adopted as the input features to expand the parameter space. The detailed description and formula of the twelve physical features are presented in Table S1. Subsequently, the values of the features are normalized to (0,1): i) Each individual feature has the same numerical scale; ii) All features are treated equally. Furthermore, the t-stochastic neighbor embedding (t-SNE) method[23] is used to investigate the feature distribution of the whole sample in two dimension, as shown in Figure 2 (the detailed data corresponding to the each MPEA in Data S3). The original data distribution can be presented in Figure S1. There are two advantages in choosing the t-SNE method for data analysis: (i) Converting the high dimension data into low dimension space makes the data distribution to be better visualized, and each axis does not need to be given a clear physical meaning; (ii) Original information of the high dimensional feature space can be maintained. Here, there are some BCC alloys far away from other materials (the top right of Figure 2), which are mainly refractory MPEAs, such as Nb-Ta-Ti-V, Hf-Nb-Ta-Zr, and Mo-Nb-Ta-Ti-Zr systems. For the MPEAs lacking the refractory elements, like Cr-Co-Fe-Ni and Cu-Al-Cr-Co-Fe-Ni systems, they mainly locate at the left region of Figure 2. Furthermore, although the distributions of BCC and FCC phases are obviously separated, the samples of BCC+FCC phase are significantly entangled with them. This trend indicates that the feature information of them in origin high dimension space is similar. Therefore, using empirical rules to identify the phase selection is difficult.

Accordingly, in this work, the machine learning model with high efficiency and accuracy is developed to search for the nonlinear mapping that distinguishes the feature distribution of various phases. Moreover, in view of the small data size, the current machine learning model could predict accurately the phases of MPEAs, which are limited in initial data set.

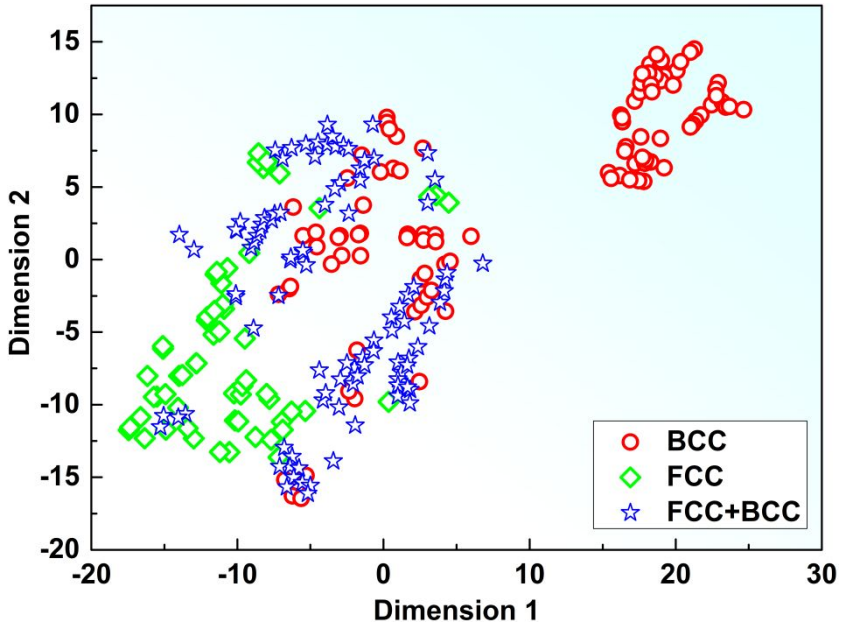

Figure 2 Feature distribution of the 266 samples in two dimensional space via t-SNE.

Phase prediction

In order to obtain the optimal features of phase predictions, removing less important features can perform more reliably in classification tasks while decreasing the size of the machine learning models. Here, a feature engineering scheme combined with the correlation analysis with physical knowledge is used to search for an optimal number of features and reduce the size of the feature space. Figure 3A shows the Pearson correlation coefficient [24] matrix for every possible input feature pair obtained from 12 features. Less than 10% of features have absolute values of correlation coefficients of larger than 0.8 (Fig. 3A), confirming the relatively-small redundancy. Further, the physics information of the features is mined to reduce the size of the feature space to an optimal number of the correlated features

(Fig. 3B). Thus, the original 12 features are converted to the 9 features resulting in a smaller feature space in the final classification process. Importantly, a more robust machine learning model can be generated by decreasing the number of features.

To select the best machine learning algorithm for phase predictions, various machine learning models are evaluated (performance of the machine learning algorithm in Supplementary Text 3). Here, the accuracy values of KNN, SVM, and DT are the average of five testing results, and the accuracy of ANN represents the average of the training, validation and testing data set, i.e., the average of the entire data set. Figure 3C indicates the comparison of the accuracy, and ANN is of potential interest for prediction performance. Meanwhile, the proposed feature engineering scheme significantly enhances the efficiency of the model without sacrificing the prediction accuracy. Moreover, for discovering the criterion on how to confirm the phase selection, the sensitivity measures for BCC, BCC + FCC, and FCC structures are calculated, respectively. The result of the trained ANN model for the sensitivity measure of the feature (Fig. 3D) illustrates that the weight coefficient of the valence electron concentration (VEC) to decide the phase structure gradually declines, accompanied by the increase of the weight coefficient of the mixing enthalpy, which breaks the traditional rule of VEC acting as only the high impact feature.[25, 26] Hence, the formation mechanism of multi-phases is extremely complex, and this result gives avenues towards the multi-mechanism criterion that beats the single rule for the precise structural design.

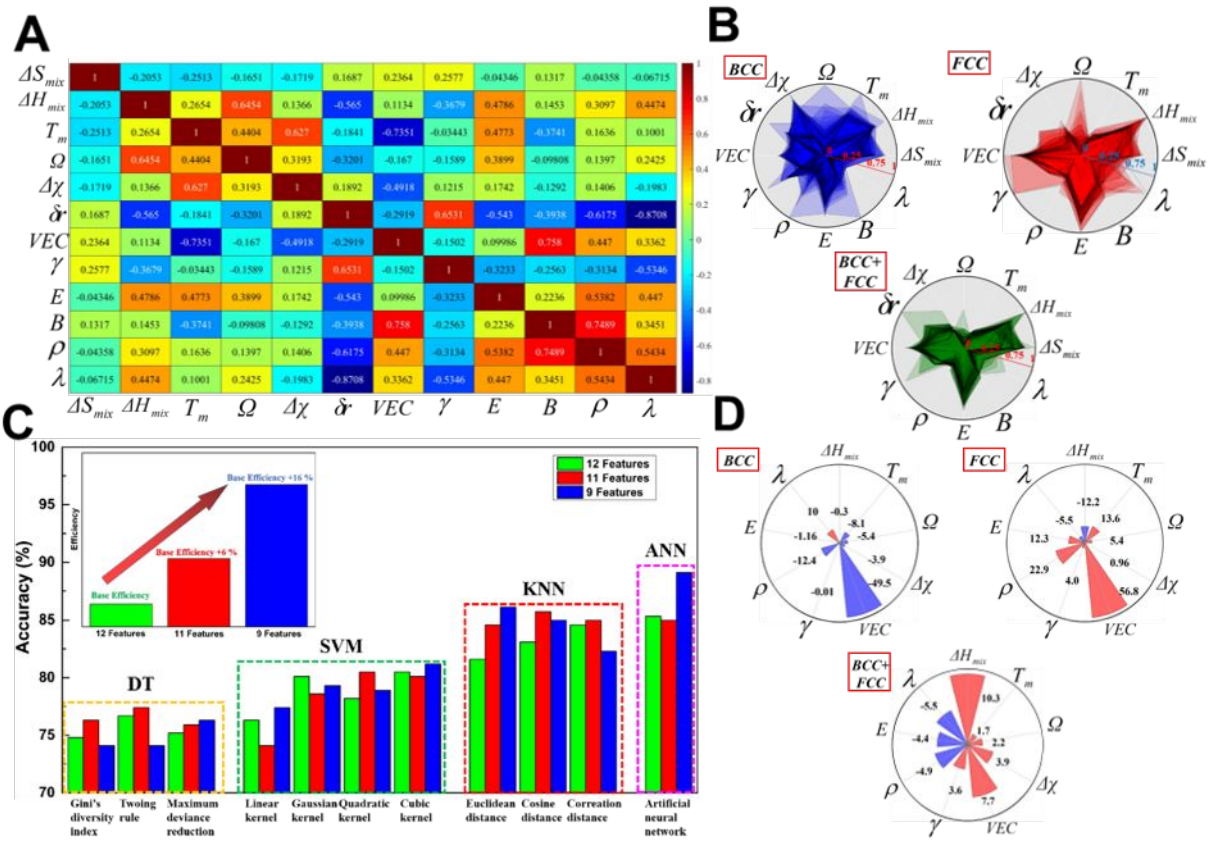

Figure 3. The correlations between the input physical features and prediction of the accuracy of machine learning models. (A) Pearson correlation coefficients for 12 features. The value in each grid represents the correlation coefficient between two features, 1 (-1) denotes the completely positive (negative) correlation, and the colour intensity reflects the magnitude of the correlation coefficient. (B) Polar charts for distributed characteristics of 12 features in BCC, BCC + FCC, and FCC phases, respectively. Area with a higher color intensity indicates the average distribution shape of the phase structure in the feature space. (C) Comparing the prediction performance using various machine learning algorithms with different training parameters. The green pillar represents the machine learning model built with 12 features, the red pillar denotes 11 features, and the blue pillar means 9 features. Based on the efficiency of the models with 12 features as benchmark efficiency, the efficiency of the model improves 16%, using the proposed feature engineering scheme. (D) The sensitivity measures with 9 features for BCC, BCC + FCC, and FCC structures via a Nightingale rose diagram. The red (blue) color represents that the sensitivity measure of the feature is positive (negative). The radius of the sector denotes the value of the magnitude of the sensitivity measure.

Yield strength of multi-phase MPEA

To accelerate the development of the complex materials, it is very common to construct the correlation among the composition, microstructure, and mechanical performance.[18] Therefore, a mathematical model is established to predict the yielding strength of the MPEA. Simultaneously, the elongation of MPEA is obtained using the machine learning approach due to lack of accurate prediction model for the ductility (Supplementary Text 4).

We have carefully curated literature data on the yield strengths of a range of MPEAs with various phase structures, including the FCC, BCC, and FCC + BCC phases. The yield strengths of the BCC and FCC MPEAs are significantly different, in which those of most FCC MPEAs are less than 400 MPa, and those of most BCC MPEAs are larger than 900 MPa (Fig. 4A). Then, the predicted strength data is compared to the experimental data, and there is a fairly-good agreement between the prediction and experiment (Fig. 4A). The further statistics indicate that the computed results with the deviation less than 3% account for 28.3%, with the deviation larger than 3% and less than 10% represent 34%, and with the deviation larger than 10% and less than 20% denote 30.2%. Specifically, only 7.5% prediction data has the deviation larger than 20%. Furthermore, it has been confirmed that the prediction accuracy of this model is superior to other typical models out of many potential candidates (Fig. 4B). This developed mathematical model interrogating the machine learning would be efficiently used as constraints to predict properties of hypothetical MPEAs when applied to data-driven materials. These results illustrate that this mathematical model possesses excellent quantitative predictive capability and universal applicability to compute the yield strengths of MPEAs. Thus, the present model can be integrated into the machine learning approach, for

further selection of MPEAs with outstanding properties by considering various aspects: multi-component, multi-phase, and multiple-strengthening mechanisms.

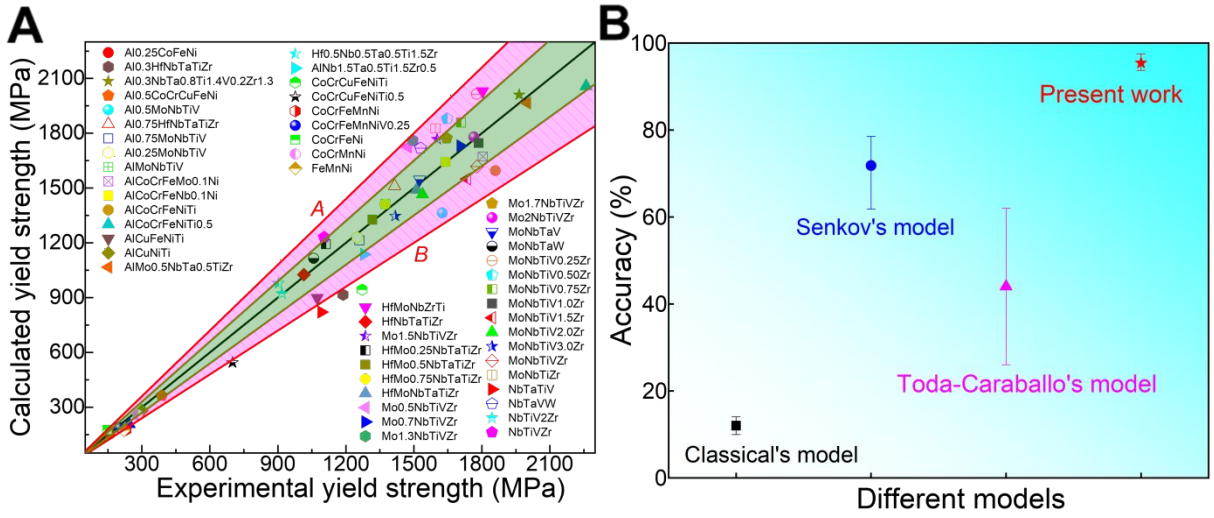

Figure 4. The strength prediction and its accuracy. (A) The deviation relationship of the yield stress between the experimental and calculated results for various MPEAs (Data S4). The black line denotes that the calculated result coincides perfectly with the experimental data. The light green area indicates that the deviation is smaller than 10%. the pink area represents that the deviation is larger than 10% but smaller than 20%, and the A and B areas denote that the deviation is larger than 20%. (B) The comparison of the prediction accuracy between the proposed model and other typical model, which is counted from various samples, including the representative FCC CrCoFeNiMn, BCC TiNbTaZrHf, and dual-phase $Al_{0.5}$CrCoFeNiMn MPEAs. The experimental data sources and modeling predictions have been provided in Table S2.

Application of multistage design strategy

The most important contribution of the current multistage design approach is to deduce the accurate element composition and phase structure. Here, the classical FeCoCrNiMn (Cantor) system is the basic principal component, and then the introduction of the Al element produces multi-phase MPEAs.[27] Meanwhile, the new $Al_{0.63}Co_{0.95}Cr_{0.95}FeMn_{0.74}Ni$ MPEA, having a good combination of strength and plasticity, has been predicted through the IP avenue in Fig.

1B (Supplementary Text 2 “Prediction of the optimal composition in the Al-Fe-Co-Cr-Ni-Mn system”). To check the validity of predictions, this alloy is prepared by arc melting. From the XRD pattern of Fig. 5A, the intensity of the peaks from FCC and BCC phases is similar, and the alloy is composed of both phases with the lattice parameters of 0.361 and 0.289 nm, respectively. To identify the crystal structures of the constitutive phases, the EBSD analysis is performed (Fig. 5B), where the estimated fractions of the FCC and BCC phases are 0.72 and 0.28, respectively. The TEM studies are performed to analyze the structure of the alloy at a nanoscale (Fig. 5C), where the existence of FCC and BCC phases is confirmed by corresponding selected area electron diffraction patterns (#1, #2, and #3 in Fig. 5C). This trend agrees reasonably well with the available literature data.[27, 28] Finally, the chemical compositions of the constitutive phases measured by the TEM-based EDS analysis is presented in Table S3. The FCC phase has the composition close to the nominal one, and the BCC phase is enriched with Cr and Fe and depleted of the rest of the elements. The tensile stress-strain curve in Fig. 5D shows a high yield strength of 880 MPa, the ultimate tensile strength of 1,235 MPa, and the elongation of 12.3%. Furthermore, the experimental results suggest that the new MPEA proposed in current work thoroughly defeats the properties of its existing system/subsystems and other MPEAs reported in previous literature,[27] as presented in Fig. 5E. The experimental strength and elongation are also located in the range of screening criteria (strength > 800 MPa and elongation > 10%, the detailed explanation is mentioned in Supplementary Text 2). Therefore, a new alloy system with excellent mechanical properties can be designed, which only takes two days, including the prediction, preparation, characterization, and performance test. These results imply the key role of our novel avenue

in designing high-performance MPEAs. Moreover, in order to further demonstrate the validity comprehensively of the proposed multistage-design approach, the $Al_{0.55}Co_{0.9}CrFe0.95Mn_{0.8}Ni_{0.8}$ MPEA with suboptimum properties has been re-selected and re-prepared. The detailed description is presented in Supplementary Text 5.

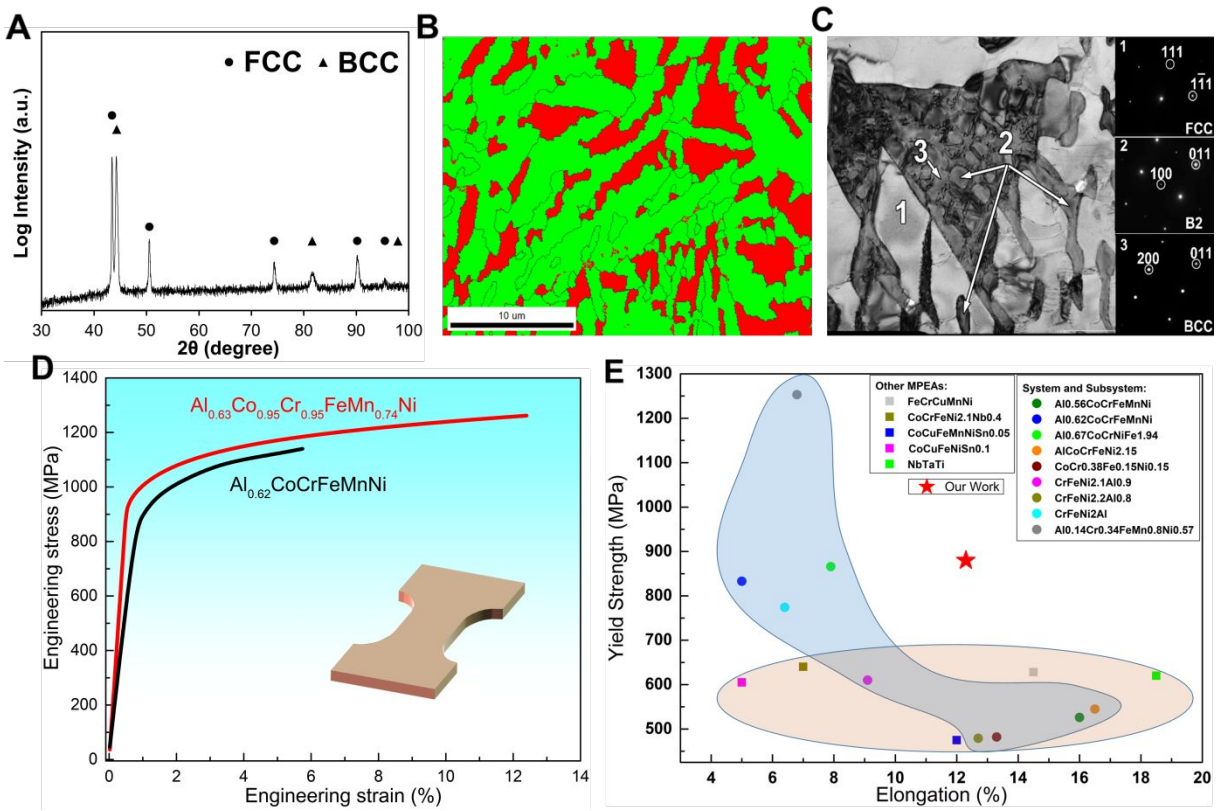

Figure 5. Results of the validation experiment. (A) Structures and mechanical properties of the as-cast $Al_{0.63}Co_{0.95}Cr_{0.95}FeMn_{0.74}Ni$ MPEA: XRD pattern. (B) EBSD phase map (the green color depicts the FCC phase, and the red denotes the BCC one). (C) TEM bright-field image with selected area electron diffraction patterns. (D) tensile stress-strain curve. (E) Ashby plot of elongation versus yield strength of the Al-Co-Cr-Fe-Ni-Mn system, and other MPEA systems (Table S4).

Comparison of design methods

The existing one-step strategy used in designing MPEAs usually attempts to directly establish the relationship from the composition to performance.[29-32] However, this mode

neglects the complex phase structure dependent upon composition, thus causing a significant deviation between the computed and target performance. For example, using one-step strategy, the AlCoCrCuFeNi MPEA with desired performance was prepared successfully at the expense of several series experimental feedbacks, due to the existence of phase transformation with the varies of Al and Cu content.[29] Moreover, the precipitation strengthened copper alloys with high properties were also obtained by the one-step strategy, but were verified by 12 experiments owing to the lack of microstructure-to-performance correlation.[30] The present work introduces the composition dominated phase structure as the intermediary, and thus realizes the multistage strategy, integrating a physics-guided machine learning to predict phase formation, and a microstructure-controlled mathematical model to calculate yield strength. Firstly, a "physics-feature-space" is constructed to describe the phase formation of MPEAs, and embed it into machine learning. Compared to the case for the composition as descriptors, the physical feature-constrained machine learning model not only contributes to accurately reveal a general criteria of phase formation (Fig. 3D), but also makes the model explainable and universal. The classical feature engineering method based on Pearson coefficient for phase prediction of MPEA has been fully reported.[24] Nevertheless, this feature analysis method is one-sided because only numerical correlations between features are assessed, causing some potential redundant features to be remain. Therefore, the proposed feature engineering method that comprehensively considers Pearson coefficient and physical features (Fig. 3B) becomes more reasonable, effectively improving the accuracy and efficiency of machine learning model (Fig. 3C). The developed mathematical model considers the extensive strengthening mechanisms, such as the grain boundary strengthening, phase

transformation strengthening, and solid solution strengthening.[33, 34] Hence, the current model is universal for multiphase MPEAs, which accuracy in the predicted strength is up to 90% and overmatches that of other existing models (Fig. 4). The robust machine learning and mathematical models are the intrinsic reason for the accuracy of this novel approach in FP avenue. Compared to the one-step strategy, the multistage strategy significantly reduces the initial composition space in IP avenue. Subsequently, FP avenue is employed to compute the performance of the initial composition space and screen out the optimal composition based on the optimal performance, avoiding a lot of experimental trial and errors and obtaining the low cost yet high efficiency using the multistage design strategy.

As well-known, the high strength of the alloy most likely stems from the multiphase microstructure (Fig. 5E). For the Al-Co-Cr-Fe-Ni-Mn system, the combination of Al and Ni tends to form the BCC phase because of the high formation enthalpy.[29] With increasing the Al content, the MPEAs transform from FCC phase to BCC + B2 phase. Thus, the multiphase enabling strength-plasticity synergy is developed, owing to the reason: the FCC matrix provides a reasonable elongation and good strain-hardening capacity, and the BCC and B2 phases are acted as a hard reinforcement and generates strong back stresses in the softer FCC phase. Our multistage strategy can capture this rule hidden, guiding the experimental exploration of multi-phase MPEAs that go beyond the limitations of conventional alloy performance. With respect to the cycle of the development for alloys, a comparison with the major technologies is presented in Fig. 6. The traditional experiments are most time and cost consuming, due to lots of trials and errors. The high-throughput, theoretical model and simulation-assisted experiments enhance efficiency (or reduce cost) to a certain extent. This is

deriving from the wide composition range space and its induced uncertainty of microstructure. The existing design strategy combining machine learning and experiments still require some trials as the feedback. Here, the cost and efficiency of the proposed approach virtually exceeds those of previous material design technologies, providing new avenue to simultaneously achieve the rapid and accurate material design.

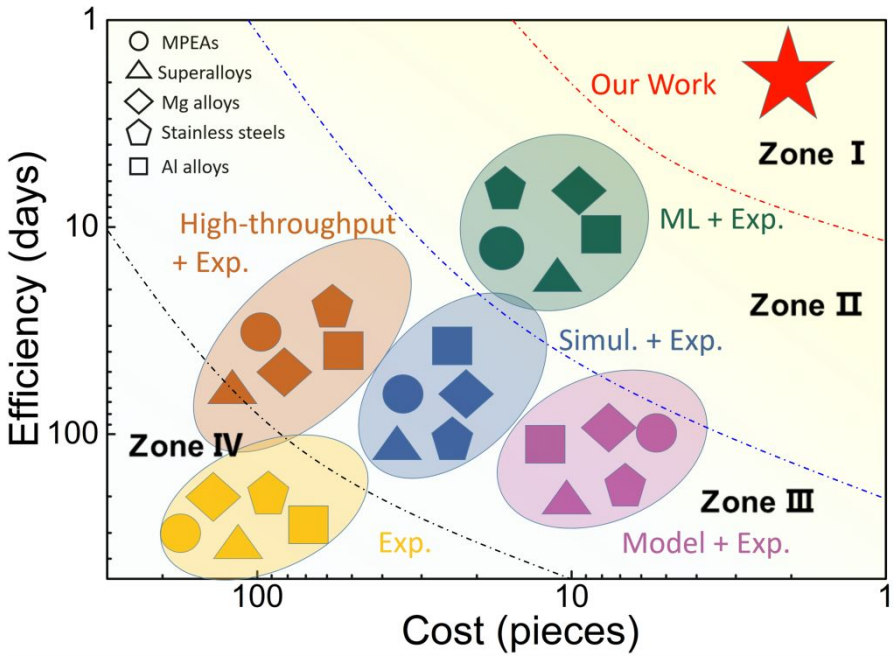

Figure 6. Advantages of the method. Ashby map showing efficiency as a function of cost and time in relation to the potential material design technologies (Table S5). Zones Ⅰ-Ⅳ represent a deteriorating combination of efficiency and cost.

In the present work, we have proposed a multistage design approach integrating machine learning, physical law, and mathematical model to achieve the rapid design for the multi-phase MPEA. Based on the proposed strategy, a new multi-phase MPEA is developed under a very short amount of time and low consumption. Importantly, the comprehensive mechanical properties outperform its system and subsystems reported previously, in which achieve the accurate design for MPEAs with high strength and ductility. It is believed that the present work provides a fundamental framework to guide the design of advanced materials

through a means of high efficiency and low cost, helpful for reducing resource consumption.

Keywords: Multi-principal element alloys; multistage design; machine learning; high efficiency; low cost

Author contributions

Q.H.F., N.S., and P.K.L. were responsible for supervision, analysis, editing, and funding acquisition. J.L., B.B.X. and L.L. carried out the machine learning and theoretical calculations. D.S. performed the experiments. B.L. and Y.L. analyzed the data. All authors discussed the results and wrote the manuscript.

Conflicts of interest

The authors declare that they have no competing interests.

Data and code availability

All data needed to evaluate the conclusions are present in the paper and/or the Supplementary Information. The code will be made available upon request.

Acknowledgements

The authors would like to deeply appreciate National Natural Science Foundation of China (12172123, 12072109, and 51871092). P.K. Liaw very much appreciates the supports from the National Science Foundation (DMR-1611180 and 1809640).

Notes and references

[1] E. P. George, D. Raabe, and R. O. Ritchie, *Nat. Rev. Mater.*, 2019, **4**, 515-534.

[2] C. Oses, C. Toher, and S. Curtarolo, *Nat. Rev. Mater.*, 2020, **5**, 295-309.

[3] T. Yang, Y. L. Zhao, Y. Tong, Z. B. Jiao, J. Wei, J. X. Cai, X. D. Han, D. Chen, A. Hu, and J. J. Kai, *Science,* 2018, **362**, 933-937.

[4] Z. Lei, X. Liu, Y. Wu, H. Wang, S. Jiang, S. Wang, X. Hui, Y. Wu, B. Gault, and P. Kontis, *Nature*, 2018, **563**, 546-550.

[5] Y. Yao, Z. Huang, P. Xie, S. D. Lacey, R. J. Jacob, H. Xie, F. Chen, A. Nie, T. Pu, and M. Rehwoldt, *Science*, 2018, **359**, 1489-1494.

[6] S. Wei, S. J. Kim, J. Kang, Y. Zhang, Y. Zhang, T. Furuhara, E. S. Park, and C. C. Tasan, *Nat. Mater.*, 2020, **19**, 1175-1181.

[7] Q. Ding, Y. Zhang, X. Chen, X. Fu, D. Chen, S. Chen, L. Gu, F. Wei, H. Bei, and Y. Gao, *Nature*, 2019, **574**, 223-227.

[8] C. Lee, G. Kim, Y. Chou, B. L. Musicó, M. C. Gao, K. An, G. Song, Y.-C. Chou, V. Keppens, and W. Chen, *Sci. Adv.*, 2020, **6**, eaaz4748.

[9] D. B. Miracle, and O. N. Senkov, *Acta Mater.*, 2017, **122**, 448-511.

[10] M.-X. Li, S.-F. Zhao, Z. Lu, A. Hirata, P. Wen, H.-Y. Bai, M. Chen, J. Schroers, Y. Liu, and W.-H. Wang, *Nature*, 2019, **569**, 99-103.

[11] R. Singh, A. Sharma, P. Singh, G. Balasubramanian, and D. D. Johnson, *Nat. Comput. Sci.*, 2021, **1**, 54-61.

[12] Z. Wu, R. Ahmad, B. Yin, S. Sandlöbes, and W. A. Curtin, *Science*, 2018, **359**, 447-452.

[13] Z. Zhou, Y. Zhou, Q. He, Z. Ding, F. Li, and Y. Yang, *npj Comput. Mater.*, 2019, **5**, 1-9.

[14] J. M. Rickman, H. M. Chan, M. P. Harmer, J. A. Smeltzer, C. J. Marvel, A. Roy, and G. Balasubramanian, *Nat. Commun.*, 2019, **10**, 1-10.

[15] L. J. Santodonato, P. K. Liaw, R. R. Unocic, H. Bei, and J. R. Morris, *Nat. Commun*., 2018, **9**, 1-10.

[16] G. E. Karniadakis, I. G. Kevrekidis, L. Lu, P. Perdikaris, S. Wang, and L. Yang, *Nat. Rev. Phys*., 2021, **3**, 422-440.

[17] J. L. Lansford, and D. G. Vlachos, *Nat. Commun*., 2020, **11**, 1-12.

[18] J. Fish, G. J. Wagner, and S. Keten, *Nat. Mater*., 2021, **20**, 774-786.

[19] Y. Zhang, Y. J. Zhou, J. P. Lin, G. L. Chen, P. K. Liaw, *Adv. Eng. Mater*., 2008, **10**, 534-538.

[20] X. Yang and Y. Zhang, *Mater. Chem. Phys.,* 2012, **132**, 233-238.

[21] Z. Wang, Y.Huang, Y. Yang, J. Wang and C.T. Liu, *Scr. Mater.,* 2015, **94**, 28-31.

[22] A. K. Singh, N. Kumar, A. Dwivedi and A. Subramaniam, *Intermetallics,* 2014, **53**, 112-119.

[23] S. Y. Lee, S. Byeon, H. S. Kim, H. Jin, S. Lee, *Mater. Des.,* 2021, **197**, 109260.

[24] Z. Pei, J. Yin, J. A. Hawk, D. E. Alman and M.C. Gao, *npj Comput. Mater.,* 2020, **6**, 1-8.

[25] R. Chen, G. Qin, H .Zheng, L. Wang, Y. Su, Y. Chiu, H. Ding, J. Guo and H. Fu, *Acta Mater.,* 2018, **144**, 129-137.

[26] V. Chaudhary R. Chaudhary, R. Banerjee, and R. V. Ramanujan, *Mater. Today,* 2021, **49**, 231-252.

[27] J. Y. He, W. H. Liu, H. Wang, Y. Wu, X. J. Liu, T. G. Nieh and Z.P. Lu, *Acta Mater.,* 2014, 62, 105-113.

[28] N. D. Stepanov, D. G. Shaysultanov, R. S. Chernichenko, M. A. Tikhonovsky, and S.V. Zherebtsov, *J. Alloys Compd.,* 2019, **770**, 194-203.

[29] C. Wen, Y. Zhang, C. Wang, D. Xue, Y. Bai, S. Antonov, L. Dai, T. Lookman and Y. Su, *Acta Mater.,* 2019, **170**, 109-117.

[30] H. Zhang, H. Fu, S. Zhu, W. Yong, and J. Xie, *Acta Mater.,* 2021, **215**, 117118.

[31] W. Wan, X. Jiang, S. Tian, P. Liu, D. Dang, Y. Su, T. Lookman, J. Xie, *npj Comput. Mater.,* 2022, **8**, 1-12.

[32] B. Xiong, X. Zhao, Y. Hu, H. Huang, Y. Liu, and Y. Su, *Mater. Des.,* 2021, **210**, 110037.

[33] B. Yin, S. Yoshida, N. Tsuji and W.A. Curtin, *Nat. Commun.,* 2020, **11**, 1-7.

[34] C. Varvenne, A. Luque and W. A. Curtin, *Acta Mater.,* 2016, **118**, 164-176.